



Compaction mechanics of a polydisperse crushable spherical granular assembly using discrete element method

Raghuram Karthik Desu¹ · Yixiang Gan² · Marc Kamlah³ ·
Ratna Kumar Annabattula⁴

Accepted: 9 December 2020 / Published online: 4 February 2021
© Indian Institute of Technology Madras 2021

Abstract The macroscopic behaviour of an assembly of polydisperse spherical particles is studied using a numerical model based on discrete element method (DEM), which accounts for the microscopic interactions between individual particles and their damage. DEM models particle–particle interactions enabling to understand the influence of microscopic particle–particle interactions on the macroscopic response. The method is used to stimulate the mechanical response of a polydisperse particle assembly under uniaxial compressive load. The influence of damage rate and the initial packing fraction on the macroscopic stress–strain response is investigated. The analysis shows that the initial nonlinear elastic behaviour is influenced by the initial packing factor, whereas the critical stress is influenced by both initial packing fraction and damage rate. It is also observed that critical stress occurs when the assembly reaches a particular damage state. Furthermore, the failure behaviour of different sized particles within a polydisperse assembly is also investigated. The experimental data from the literature show that the crush strength of the particle of given size is observed to vary over a

range. Such variation of crush strengths for a given particle size is also implemented in the present work.

Keywords Crushing · Polydispersed granular assembly · Discrete element method

1 Introduction

The mechanical behaviour of a granular assembly is not only influenced by the bulk properties of the constituent particles but also by various other factors, viz. topology of the particle arrangement, packing fraction, relative radii and size distribution of the particles in the assembly [1–5]. Unlike the solid systems, granular systems behave differently due to their discrete nature. Understanding their mechanical response is important for designing the systems involving granular subsystems to ensure the structural integrity for smooth and continuous operation. Granular systems have been studied under two methods, phenomenological modelling and modelling based on individual pebble–pebble interactions. The later is aimed at investigating the micro-scale interactions at the particle level to relate with the macroscopic response of the granular system. Discrete element method (DEM), a numerical model based on particle–particle interactions, is used to understand the mechanical response for an assembly of crushable spherical pebbles. DEM models particle–particle interactions enabling to deduce the relation between the microscopic interactions to the macroscopic response. The discrete element method is an effective way to study the micromechanical behaviour of granular systems in many engineering fields [6].

In fusion reactors, lithium (Li) ceramic pebbles and beryllium pebble beds work as tritium breeder and neutron

✉ Raghuram Karthik Desu
desu@nitt.edu

¹ Department of Mechanical Engineering, National Institute of Technology Tiruchirappalli, Trichy 620015, India

² School of Civil Engineering, The University of Sydney, Sydney, NSW 2006, Australia

³ Institute for Applied Materials (IAM-WBM), Karlsruhe Institute of Technology, 76344 Eggenstein-Leopoldshafen, Germany

⁴ Department of Mechanical Engineering, Indian Institute of Technology, Madras, Chennai 600036, India

multiplier, respectively. DEM helps to understand interactions at the particle level so as to establish a relation with the macroscopic response of the particle assembly subjected to external load. There have been studies done on binary pebble assemblies assuming the particles to be elastic [7]. But in reality, the ceramic pebbles are brittle and prone to failure. Some of the recent studies [7, 8] have considered the crushing behaviour of monosized particle assemblies by incorporating certain damage laws. However, the pebble (Li) production process results in a large variation of pebble sizes in a batch. This leads to the rejection of a significant fraction of pebbles to maintain monosize pebble assemblies. Hence, it is worth investigating the response of polydisperse pebble assemblies to establish their suitability for the breeder units. Hence, in this paper, crushable polydisperse assemblies are studied to investigate the influence of initial packing fraction (η) and size distribution on the crushing behaviour of the pebbles in the assembly. The effect of aforementioned parameters on the macroscopic stress–strain response will also be investigated. This study helps in understanding the macroscopic response and damage as a function of the microscopic factors paving a way to develop a predictive model for estimating failure conditions in a brittle granular assembly with polydisperse particle sizes.

The outline of the papers is as follows. In Sect. 2, the simulation model and different parameters employed in the simulations are presented. In Sect. 3, the results concerning the influence of damage and packing are discussed for the polydisperse assembly, followed by monosized pebble assembly response, and Sect. 4 presents conclusive remarks.

2 Description of the model

A pebble assembly consisting of 5000 spherical particles is considered as a representative volume element (RVE) with periodic boundary conditions (Fig. 1). Typically, the thermo-mechanical response of a pebble bed is characterized by the (uniaxial) oedometric compression tests [9–11]. Hence, the considered assembly is subjected to uniaxial compression in Z-direction up to a macroscopic strain of 1.5% and then unloaded to a stress-free state. The pebbles are taken to be spherical, with an elastic modulus of 90 GPa and Poisson's ratio of 0.25 (properties of lithium orthosilicate (OSi) [12]). The diameter of the OSi pebbles has been reported to vary from 0.25 to 0.8 mm (Fig. 2), and their size distribution is taken as per the pebbles produced by L bbecke and Knitter [13].

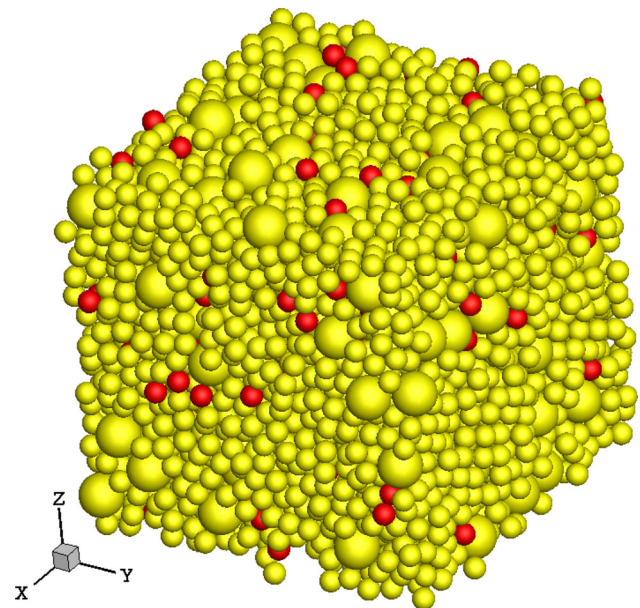


Fig. 1 Representative volume element of the pebble assembly showing the damaged pebbles (red) (color figure online)

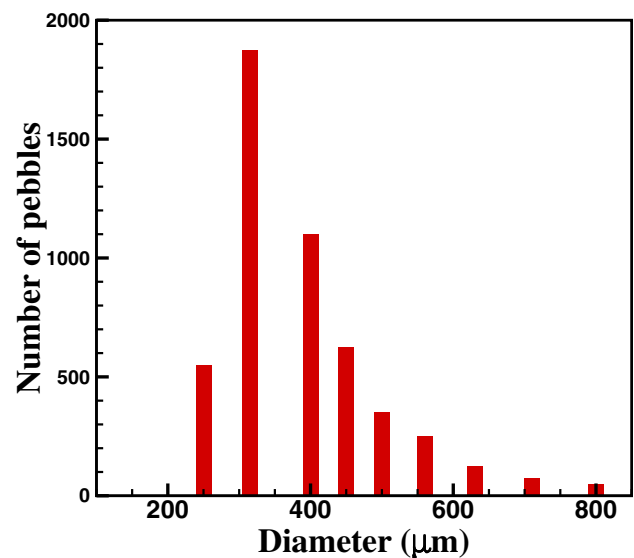


Fig. 2 Size distribution of the pebbles in polydisperse assembly [13]

2.1 Crush energies

Experimental investigations of Zhao [14] show that pebbles of the same radius fail at different loads (crush loads), due to variable defect density and pore structure within the pebble. The variation of crush load for a given pebble radius is observed to follow a Weibull distribution [14, 15]. Pebbles of the same radius have different crush loads distributed over a range, and the span of the range changes with the particle size [14, 16]. The OSi pebbles have shown an increase in average crush load as the pebble size

increases. The crush loads are expressed in terms of the energies (crush energies) [16]. Figure 3 shows the cumulative probability of the critical (crush) energy of the pebbles for various radii. The crush energies of the pebbles can be described through a Weibull distribution given by

$$W_C = \alpha \sqrt[\beta]{\ln\left(\frac{1}{1-P}\right)} \quad (1)$$

where W_C is the crush energy (μJ), α and β are the Weibull constants and P is the cumulative probability. The α and β values vary according to the size of the pebble and are evaluated from the experimental crush energies for various radii (see Table 1). The RVE consisting of a polydisperse assembly with a radius distribution (Fig. 2) is considered for the simulation. As mentioned earlier, the crush energy of a pebble for a given radius is not a unique value but varies over a range. Each and every particle in the RVE has to be assigned with a particular crush energy within the observed crush range corresponding to the particle size. The assignment of the crush energies is done by assigning each particle a random value of cumulative probabilities (P in Eq. 1) irrespective of the radius and subsequently calculating the crush energy based on Eq. 1, the particle radius and their corresponding Weibull constants (Table 1). The above procedure enables a more realistic scenario for the simulation compared to assigning an average crush energy for particles of a given size. Assuming average crush values, increase the overall crush resistant of the assemblies as the minimum crush energy is raised to the average value. However, the pebble with crush energies lower than the average crush value is prone to fail early,

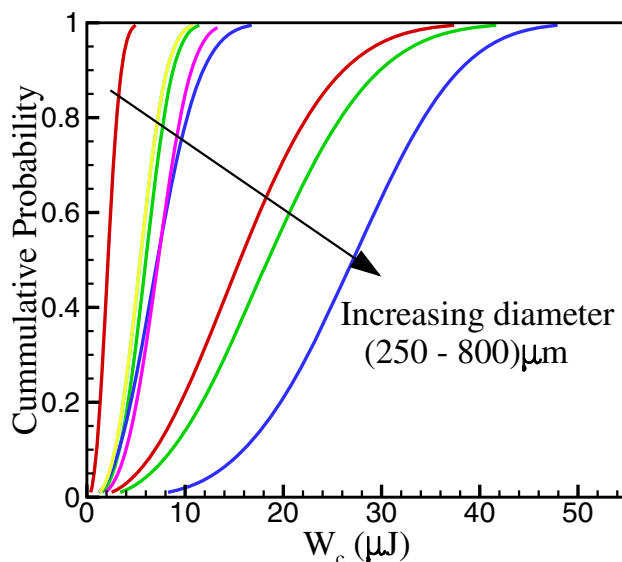


Fig. 3 Cumulative probability distribution of critical elastic energy of pebbles of different radii

Table 1 Weibull constants (α and β) for various pebble radii

Pebble radius (μm)	α	β
250	2.499	2.431
315	6.744	3.154
355	3.791	1.997
400	8.359	2.394
450	6.149	2.961
500	6.144	2.947
560	8.166	3.132
630	18.252	2.325
710	21.369	2.496
800	30.019	3.565

which cannot be captured considering average crush energies.

2.2 Damage model

The damage of pebbles can be incorporated in the simulations by various damage laws [7, 8]. A damage accumulation law, proposed by Annabattula [7] is used for accounting the damage of the individual pebbles in the present study. It is assumed that the damage is taken into account by the reduction of the elastic modulus of the pebble. Damage starts when the strain energy of a pebble (ϕ_i) reaches the failure/crush energy (ϕ_i^{cr}) (see Eqs. 2, 3). In this work, an exponential damage accumulation law is considered [7]

$$E = (1 - D_i) * E_0, \quad (2)$$

$$D_i = 1 - \exp\left(-a\left(\frac{\phi_i}{\phi_i^{\text{cr}}} - 1\right)\right), \quad (3)$$

where E_0 is the initial elastic modulus and a describes the rate at which D approaches unity. Larger value of a indicates a sudden failure analogous to brittle failure, and smaller values of a imply ductile failure behaviour of the pebble. D_i is the damage accumulation factor which is a function of ratio of strain energy to failure energy.

Simulations are carried out using an in-house DEM code (DEM_KIT) [17]. The simulations are performed for different values of a , varying from a low to high value (gradual to sudden damage) and for different packing fractions (η). In this work, three different packing fractions have been investigated. The assembly is subjected to macroscopic loading through application of strain followed by unloading to a stress-free state.

3 Results and discussion

In this section, the results of the DEM simulations for crushable polydisperse assemblies are presented. The effect of damage criteria and packing fraction on macroscopic response and failure of individual pebble are presented as follows. The normal stress developed in the direction of loading (Z-direction) is referred to as stress, and average of the normal stress in X, Y and Z directions is termed as the hydrostatic stress. Hydrostatic stress is chosen as one of the parameters as it is the first invariant of the stress tensor.

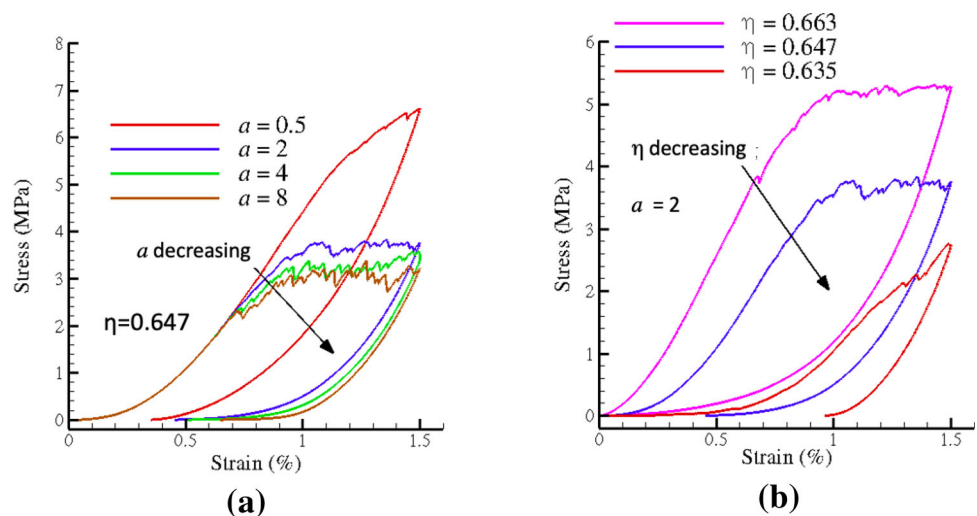
Figure 4 shows the macroscopic stress–strain response for various damage constants (a) for a polydisperse pebble assembly. The pebble size distribution and crush energies are considered as mentioned earlier. The damage constant is varied from a gradual damage ($a = 0.5$) to sudden damage ($a = 8$). From Fig. 4, it is observed that the damage constant has shown a significant effect on the overall response of the system. The stress–strain response shows initial nonlinear elastic response followed by the plateau formation occurring due to failure of pebbles. The initial elastic path is traced same for the different cases until the onset of failure in the system. The stress plateau is due to the subsequent continuous failure of more pebbles. The critical stress, defined as stress value where the plateau forms, is observed to decrease as the a value increases. The reduction in critical stress is in direct correlation with damage law which follows an exponential decrease with linear increase in a value. The plateau formation is occurring almost at the same strain independent of a value from $a > 2$. The residual stress after unloading can also seen to depend on the extent of damage which is governed by the value of a . For higher values of a , the assembly is prone to more damage resulting in higher residual strain.

Figure 4b shows the effect of initial packing fraction (η) on the macroscopic stress–strain response. The systems

with higher initial packing fraction are stiffer as seen from Fig. 4b. It is observed that the critical stress value (plateau formation) is decreasing with reduction in the packing fraction. For higher and medium η values, failure of pebbles is followed by attaining the critical stress value, whereas for low η , we observe strain hardening like behaviour due to occurrence of both rearrangement and crushing simultaneously. For loosely packed system, due to rearrangements the crush events are delayed, viz. formation of plateau. It is also seen that no significant stress develops even when the strain is 0.5%. The rearrangement is enhanced by the ball-bearing effect between smaller and bigger pebbles, making it easy. The final bed strain is increasing with decreasing initial η , due to irreversible rearrangements of particles.

A monosize pebble assembly equivalent to polydisperse crushable assembly has been investigated. The equivalent monosized assembly has the pebble radius equivalent to the average radius in the polydisperse assembly, both have the same packing fractions, implying equivalent volume. From Fig. 5, we can clearly observe a significant effect of size distribution on the stress response of the system. The monoequivalent is having a high stiffness compared to the polydisperse assembly of same initial η . For the monoequivalent assemblies, critical stress is higher stress compared to its corresponding equivalent polydisperse pebble assembly. The polydisperse assembly is having a higher residual bed strain compared to monosized even though both have same initial η . The reason is being due to the easy movement and rearrangement ability of pebbles in polydisperse assembly. For a moderate and high η values the plateau formation is almost occurring at the same strain value for monoequivalent and polydisperse but at different stress values.

Fig. 4 Macroscopic stress–strain response for a pebble assembly for: (a) packing fraction of 0.6473 for different damage constants (a) and (b) damage constant a of 2 for different initial packing fractions



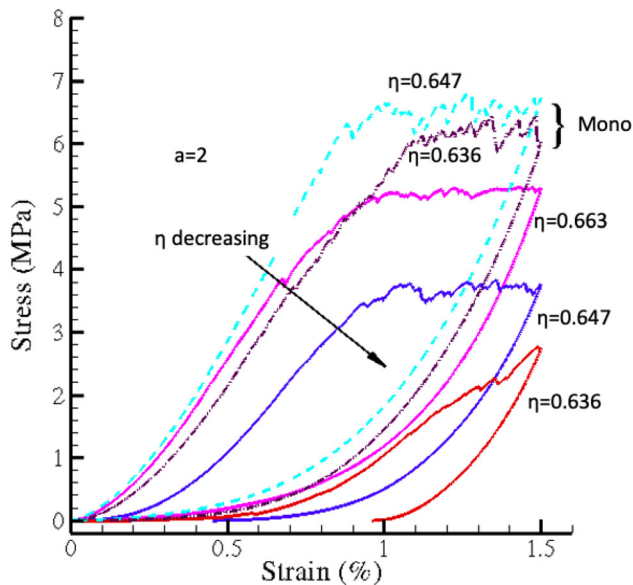


Fig. 5 Macroscopic stress–strain response of monosized and polydisperse pebble assembly

In order to estimate and compare the damage of different systems, we have quantified the damage in terms of damaged volume percentage, given by

$$D_V(\%) = \frac{\sum_{i=1}^N D_i * V_i}{\sum_{i=1}^N V_i} * 100, \quad (4)$$

where V_i is the volume and D_i is damage of the i th particle and N is the total number of pebbles in the assembly. Figure 6 shows the evolution of damage (solid lines) in the assembly as a function of strain, along with the stress response (dashed lines). The plateau formation is occurring in the damage range of 0.5–1%. This value is towards 1% for the monosized assembly. The damage value in Fig. 6b

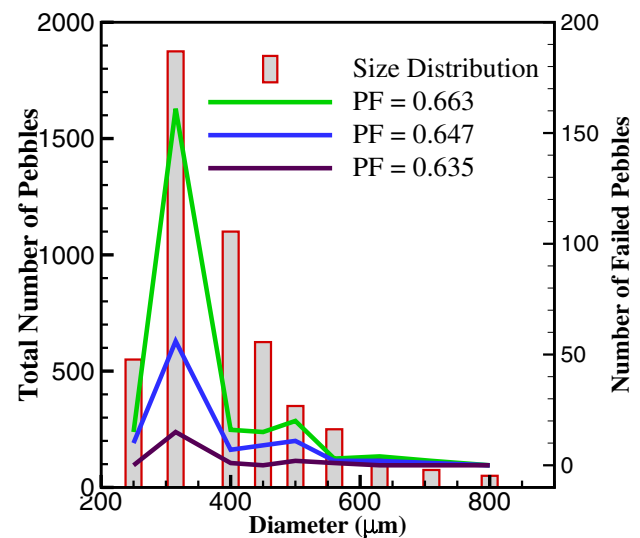


Fig. 7 Size distribution of the pebbles and number of failure pebbles at the end of 1.5% strain ($a = 2$). The bar shows the total number, and the lines indicate number of failed pebbles

for polydisperse has not crossed 0.5%, implying the stress has not reached the critical stress value which can be seen in Fig. 6b. In monosized pebble assembly, the damage seems to be occurring at faster rate once the critical stress is reached, as most pebbles have attained their critical energy.

Figure 7 shows the number of failed pebbles (lines) at the end of the loading the assembly along with the pebble size distribution (histogram) for various initial packing fractions. It can be observed that for a given loading strain (1.5% in present case), assemblies with initial higher packing fraction have larger number of damaged pebbles as seen from Fig. 7. Higher initial η implies a compacted assemblies with less scope for rearrangements; hence, at a

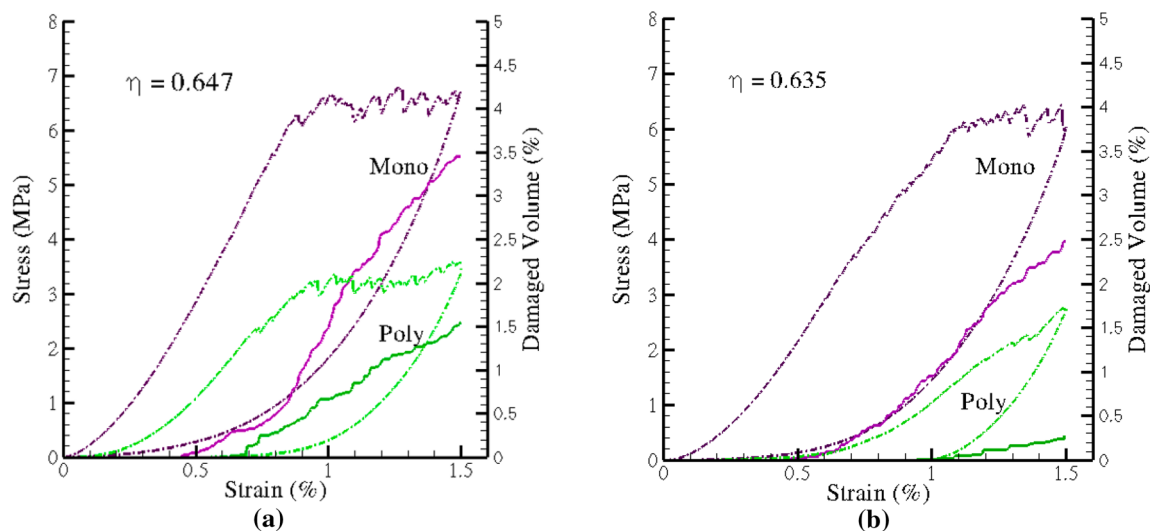


Fig. 6 Macroscopic stress response and damaged volume (%) as a function of strain for various mono- and polydispersed systems for $a = 2$

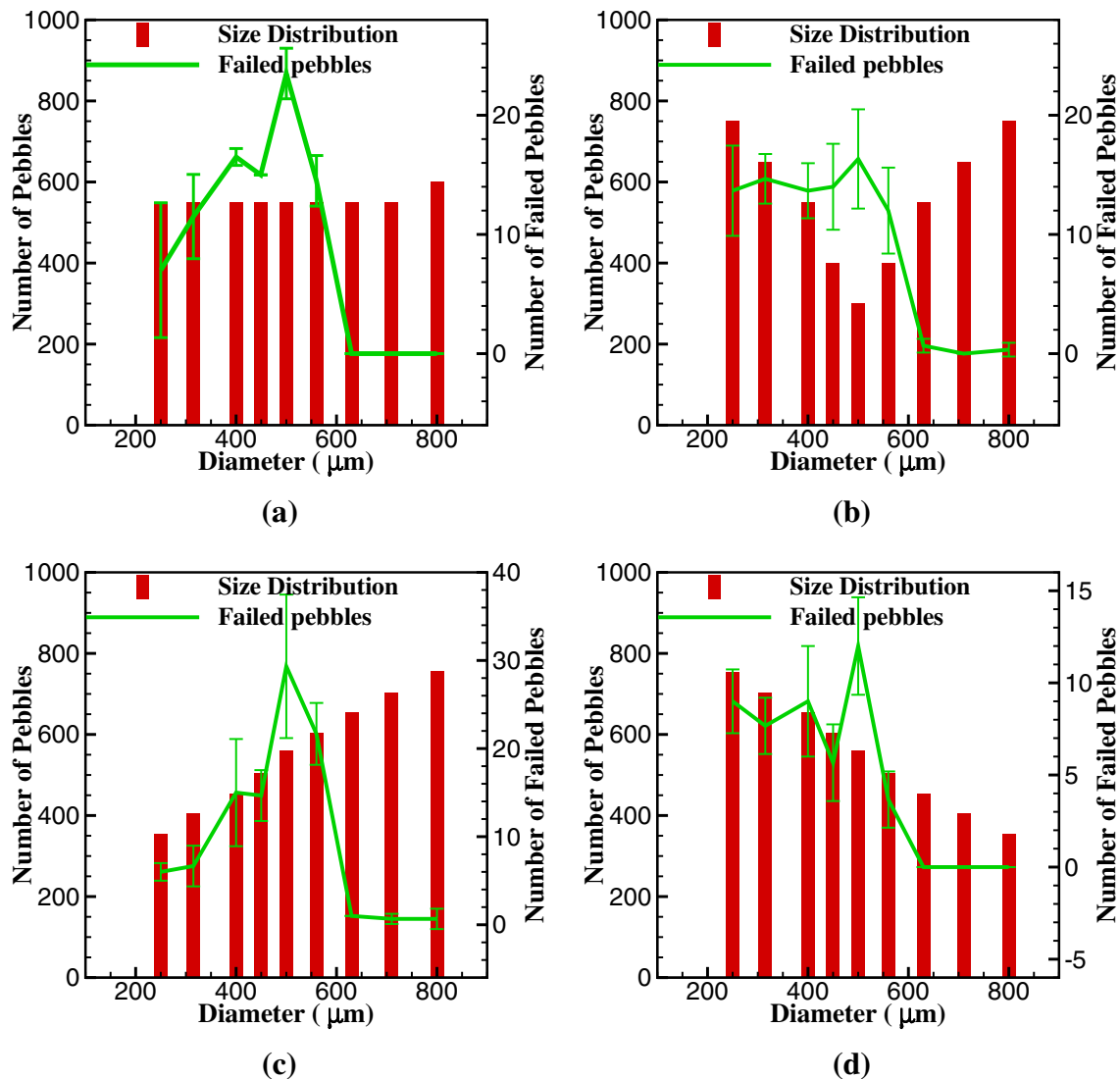


Fig. 8 Size distribution of the pebbles and number of failure pebbles at the end of 1.5% strain ($a = 2$)

lower strain the system develops higher stress compared to less compacted assembly (lower initial η). The distribution of the failed pebbles with respect to size is observed to remain almost same as that of overall pebble-size distribution of the assembly (comparing the bar graph and line graph trend). The present pebble-size distribution has more smaller size pebbles, and also their crush energies are low as seen from Fig. 3, and hence, there is a greater possibility for failure and is evident from Fig. 7. The low critical stress in the polydisperse assembly (Fig. 5) compared to the monosized pebbles can be due to the failure of smaller pebbles (as seen in Fig. 7 where a large number of smaller pebbles failed) which have lower crush energy compared to the average crush energy considered for the monosized assemblies.

In order to understand the failure behaviour with respect to the pebble size distribution in the assembly, few

simulations are carried out for various cases of pebble size distributions. Figure 8 shows the various size distributions and their respective failed pebbles at the end of 1.5% strain. For an uniform distribution (number of particles) as seen in Fig. 8a, medium-sized (relative to distribution) pebbles have failed more in number compared to smaller and larger ones. For the case of larger pebbles, this may be due to their higher crush energies resulting in withstanding higher loads are less prone to failure. However, the smaller pebbles, having lower crush energies, are more prone to failure and should have resulted in larger number of failed pebbles. However, medium-sized pebbles have seen to be failed in large number. This is also observed in other distributions also as seen in Fig. 8a–d. Even when the smaller pebbles are more in number (see Fig. 8d) compared to medium-sized pebbles, the relative damage is seen more in medium-sized pebbles. As far as larger pebbles are

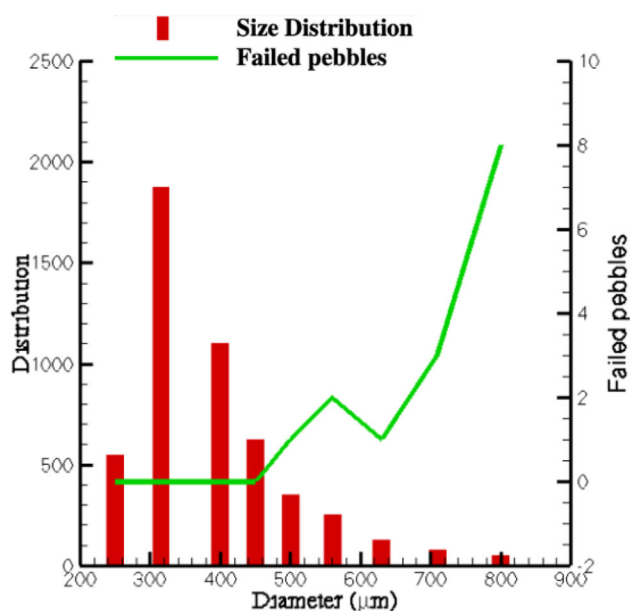


Fig. 9 Size distribution of the pebbles (histogram) and number of failure pebbles (line) at the end of 1.5% strain ($a = 2$), for pebbles having identical crush energies irrespective of size

considered, the damage is seen low due to their high load-carrying capacity. The observation shows that the forces are not uniformly distributed among all the particles and influenced by the relative sizes. A special hypothetical case is considered to study the force distribution among the pebbles of different sizes. The simulation is carried for three different realisations for each case and has observed similar trends as shown in Fig. 8 (error bars).

A polydisperse assembly with the initial size distribution (Fig. 2) is considered for the study. All the pebbles irrespective of the size have assigned same crush energy (hypothetical case). As all the particles are assigned with same crush energy, the relative failed pebbles indicate the relative force distribution among different sizes in the assembly. Figure 9 shows the distribution of failed pebbles at the end of loading. It is observed that the failure is highly dominated by the size, indicating that the load is distributed more on larger-sized pebbles. Hence, it can be concluded that the failure of the pebbles is not just a function of relative crush energies but also depends on the force distribution in the assembly. The force distribution among particles of different size is observed to be a function of not only pebble sizes but also relative number of pebbles in the assembly [18]. The relative sizes play an important role in the distribution of forces among different sized particles, governing the failure of the particles. The smaller particles are seen to carry lower load or no load resulting in lower failure. The relatively small-sized particles escape the load by occupying the voids created by the larger particles. Similar force distribution among different sizes in

polydisperse assembly has been reported by Desu and Annabattula [18].

4 Conclusions

In summary, we have investigated the behaviour of a polydisperse pebble assembly under the application of uniaxial compression allowing the pebbles to damage in the process. We used a numerical model based on DEM to simulate the compression and to understand the behaviour, especially the influence of initial packing fraction and the damage rate. The results show that the stress–strain response is influenced by these factors significantly. The critical stress is influenced significantly by damage rate and also on the packing fraction (η). The initial nonlinear elastic response in the stress–strain curve is mostly influenced by the initial packing fraction (η) of the assembly. We have also observed that the critical stress is occurring when the damage value is around 0.5% to 1%, not being influenced by the initial η . The assembly's pebble size distribution, crush energies and packing fraction are influencing the distribution of the failed pebbles in the assembly. The failure of the particle is a function of crush energies and their relative size in the polydisperse assembly. The relative size distribution of particles is seen to govern the distribution of external load. The particle radius also results in the variation of the crush energies (for the present case). The interplay between these two quantities governs the failure in the polydisperse system.

Compliance with ethical standards

Conflict of interest The authors declare that they have no conflict of interest

References

1. Papeschi, S., Knitter, R., Kamlah, M.: Effective thermal conductivity of advanced ceramic breeder pebble beds. *Fusion Eng. Des.* **116**, 73–80 (2017)
2. Reimann, J., Hermsmeyer, S.: Thermal conductivity of compressed ceramic breeder pebble beds. *Fusion Eng. Des.* **61**, 345–351 (2002)
3. Moscardini, M., Gan, Y., Papeschi, S., Kamlah, M.: Discrete element method for effective thermal conductivity of packed pebbles accounting for the Smoluchowski effect. *Fusion Eng. Des.* **127**, 192–201 (2018)
4. Piazza, G., Jörg Reimann, E., Günther, R.K., Roux, N., Lulewicz, J.D.: Characterisation of ceramic breeder materials for the helium cooled pebble bed blanket. *J. Nucl. Mater.* **307**, 811–816 (2002)
5. Peeketi, Akhil Reddy, Moscardini, Marigrazia, Vijayan, Akhil, Gan, Yixiang, Kamlah, Marc, Annabattula, Ratna Kumar: Effective thermal conductivity of a compacted pebble bed in a stagnant gaseous environment: An analytical approach together with DEM. *Fusion Eng. Des.* **130**, 80–88 (2018)

6. Cundall, P.A., Strack, O.D.L.: A discrete numerical model for granular assemblies. *Geotechnique* **29**(1), 47–65 (1979)
7. Annabattula, R.K., Gan, Y., Zhao, S., Kamlah, M.: Mechanics of a crushable pebble assembly using discrete element method. *J. Nucl. Mater.* **430**, 90–95 (2012)
8. Lew, V., Jon, T., Ying, A., Abdou, M.: A discrete element method study on the evolution of thermomechanics of a pebble bed experiencing pebble failure. *Fusion Eng. Des.* **89**(7), 1151–1157 (2014)
9. Gan, Y., Kamlah, M.: Discrete element modelling of pebble beds: with application to uniaxial compression tests of ceramic breeder pebble beds. *J. Mech. Phys. Solids* **58**(2), 129–144 (2010)
10. Ying, A., Akiba, M., Boccaccini, L.V., Casadio, S., Dell’Orco, G., Enoda, M., Hayashi, K., Hegeman, J.B., Knitter, R., van der Laan, J., et al.: Status and perspective of the R&D on ceramic breeder materials for testing in ITER. *J. Nucl. Mater.* **367**, 1281–1286 (2007)
11. Reimann, J., Boccaccini, L., Enoda, M., Ying, A.Y.: Thermo-mechanics of solid breeder and Be pebble bed materials. *Fusion Eng. Des.* **61**, 319–331 (2002)
12. Zaccari, N.: Aquaro, donato: mechanical characterization of Li_2TiO_3 and Li_4SiO_4 pebble beds: experimental determination of the material properties and of the pebble bed effective values. *Fusion Eng. Des.* **82**(15), 2375–2382 (2007)
13. Löbbbecke, B., Knitter, R.: Procurement and quality control of Li_4SiO_4 pebbles for testing of breeder unit mock-ups. Report on TW6-TTBB-006-D2, FZK Fusion (2007)
14. Zhao, S.: Multiscale modeling of thermomechanical properties of ceramic pebbles. Ph.D. Thesis, Karlsruhe Institute of Technology (2010)
15. Desu, R.K., Chaudhuri, P., Annabattula, R.K.: High temperature oedometric compression of Li_2TiO_3 pebble beds for Indian TBM. *Fusion Eng. Des.* **136**, 945–949 (2018)
16. Annabattula, R.K., Kolb, M., Gan, Y., Rolli, R., Kamlah, M.: Size-dependent crush analysis of lithium orthosilicate pebbles. *Fusion Sci. Technol.* **66**, 136–141 (2014)
17. Gan, Y., Kamlah, M., Reimann, J.: Computer simulation of packing structure in pebble beds. *Fusion Eng. Des.* **85**(10–12), 1782–1787 (2010)
18. Desu, R.K., Annabattula, R.K.: Particle size effects on the contact force distribution in compacted polydisperse granular assemblies. *Granul. Matter* **21**(2), 29 (2019)

Publisher’s Note Springer Nature remains neutral with regard to jurisdictional claims in published maps and institutional affiliations.